

## SIN and SIS tunneling in cuprates

Ar. Abanov and Andrey V. Chubukov

*Department of Physics, University of Wisconsin, Madison, Wisconsin 53706*

(Received 11 January 2000)

We calculate the superconductor/insulator/normal-metal (SIN) and superconductor/insulator/superconductor (SIS) tunneling conductances for the spin-fermion model. We argue that at strong spin-fermion coupling, relevant to cuprates, both conductances have dip features near the threshold frequencies when a tunneling electron begins emitting propagating spin excitation. We argue that the resonance spin frequency measured in neutron scattering can be inferred from the tunneling data by analyzing the derivatives of SIN and SIS conductances.

The electron tunneling experiments are powerful tools to study the spectroscopy of superconductors. These experiments measure the dynamical conductance  $dI/dV$  through a junction as a function of applied voltage  $V$  and temperature.<sup>1,2</sup> For superconductor/insulator/normal-metal (SIN) junctions, the measured dynamical conductance is proportional to the electron density of states (DOS) in a superconductor  $N(\omega) = -(1/\pi) \int dk \text{Im} G(k, \omega)$  at  $\omega = eV$ .<sup>3</sup> For superconductor/insulator/superconductor (SIS) junctions, the conductance  $dI/dV \propto G(\omega = eV)$ , where  $G(\omega) = \int_0^\omega d\Omega N(\omega - \Omega) \partial_\Omega N(\Omega)$  is proportional to the derivative over voltage of the convolution of the two DOS.<sup>3</sup>

For conventional superconductors, the tunneling experiments have long been considered one of the most relevant methods for the verification of the phononic mechanism of superconductivity.<sup>4</sup> In this paper we discuss to which extent the tunneling experiments on cuprates may provide the information about the pairing mechanism in high- $T_c$  superconductors. More specifically, we discuss the implications of the spin-fluctuation mechanism of high-temperature superconductivity on the forms of SIN and SIS dynamical conductances.

The spin-fluctuation mechanism implies that the pairing between electrons is mediated by the exchange of their collective spin excitations peaked at or near the antiferromagnetic momentum  $Q$ . This mechanism yields a  $d$ -wave superconductivity,<sup>6</sup> and explains<sup>5,7</sup> a number of measured features in superconducting cuprates, including the peak/dip/hump features in the angle-resolved photoemission spectroscopy (ARPES) data near  $(0, \pi)$ ,<sup>8</sup> and the resonance peak below  $2\Delta$  in the inelastic neutron-scattering data.<sup>9</sup> Moreover, in the spin-fluctuation scenario, the ARPES and neutron features are related: the peak-dip distance in ARPES equals the resonance frequency in the dynamical spin susceptibility.<sup>7</sup> This relation has been experimentally verified in optimally doped and underdoped Y-Ba-Cu-O and optimally doped Bi2212 materials.<sup>10</sup> Here we argue that the resonance spin frequency can also be inferred from the tunneling data by analyzing the derivatives of SIN and SIS conductances.

The SIN and SIS tunneling experiments have been performed on Y-Ba-Cu-O and Bi2212 materials.<sup>1,2</sup> At low/moderate frequencies, both SIN and SIS conductances display a behavior which is generally expected in a  $d$ -wave superconductor: SIN conductance is linear in voltage for

small voltages, and has a peak at  $eV = \Delta$  where  $\Delta$  is the maximum value of the  $d$ -wave gap,<sup>1</sup> while SIS conductance is quadratic in voltage for small voltages, and has a near discontinuity at  $eV = 2\Delta$ .<sup>2</sup> These features have been explained by a weak-coupling theory, without specifying the nature of the pairing interaction.<sup>11</sup> However, above the peaks, both SIN and SIS conductances have extra dip/hump features which become visible at around optimal doping, and grow with underdoping.<sup>1,2</sup> We argue that these features are sensitive to the type of the pairing interaction and can be explained in the spin-fluctuation theory.

As a warmup for the strong coupling analysis, consider first SIN and SIS tunneling in a  $d$ -wave superconductor in the weak coupling limit. In this limit, the fermionic self-energy is neglected, and the superconducting gap does not depend on frequency. For simplicity, we consider a circular Fermi surface for which  $\Delta_k = \Delta \cos 2\phi$ .

We begin with the SIN tunneling. Integrating  $G(k, \omega) = (\omega + \epsilon_k)/(\omega^2 - \epsilon_k^2 - \Delta_k^2)$  over  $\epsilon_k = v_F(k - k_F)$  we obtain

$$N(\omega) = \text{Re} \frac{\omega}{2\pi} \int_0^{2\pi} \frac{d\phi}{\sqrt{\omega^2 - \Delta^2 \cos^2(2\phi)}} \\ = \frac{2}{\pi} \begin{cases} K(\Delta/\omega) & \text{for } \omega > \Delta \\ (\omega/\Delta)K(\omega/\Delta) & \text{for } \omega < \Delta, \end{cases} \quad (1)$$

where  $K(x)$  is the elliptic integral. We see that  $N(\omega) \sim \omega$  for  $\omega \ll \Delta$  and diverges logarithmically as  $(1/\pi) \ln(8\Delta/|\Delta - \omega|)$  for  $\omega \approx \Delta$ . At larger frequencies,  $N(\omega)$  gradually decreases to a frequency independent, normal-state value of the DOS, which we normalized to 1. The plot of  $N(\omega)$  is presented in Fig. 1(a).

We now turn to the SIS tunneling. Substituting the results for the DOS into  $G(\omega)$  and integrating over  $\Omega$ , we obtain the result presented in Fig. 1(b). At small  $\omega$ ,  $G(\omega)$  is quadratic in frequency, which is an obvious consequence of the fact that the DOS is linear in  $\omega$ . At  $\omega = 2\Delta$ ,  $G(\omega)$  undergoes a finite jump. This discontinuity is related to the fact that near  $2\Delta$ , the integral over the two DOS includes the region  $\Omega \approx \Delta$ , where both  $N(\Omega)$  and  $N(\omega - \Omega)$  are logarithmically singular, and  $\partial_\Omega N(\Omega)$  diverges as  $1/(\Omega - \Delta)$ . The singular contribution to  $G(\omega)$  from this region can be evaluated analytically and yields

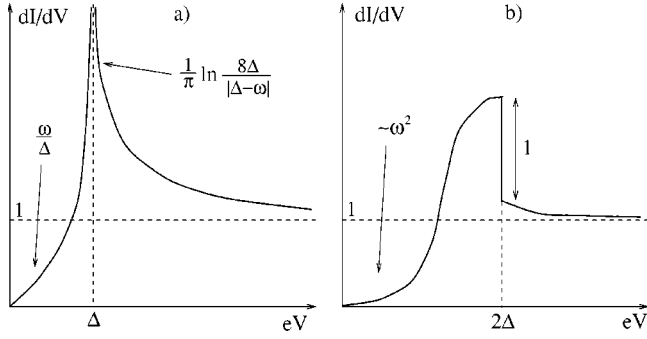


FIG. 1. The behavior of SIN and SIS tunneling conductances,  $dI/dV$ , in a  $d$ -wave BCS superconductor [(a) and (b), respectively].

$$G(\omega) = -\frac{1}{\pi^2} P \int_{-\infty}^{\infty} \frac{dx \ln|x|}{x + \omega - 2\Delta} = -\frac{1}{2} \text{sign}(\omega - 2\Delta). \quad (2)$$

We see that the amount of jump in the SIS conductance is a universal number which does not depend on  $\Delta$ .

The results for the SIN and SIS conductances in a  $d$ -wave gas agree with earlier studies.<sup>11</sup> In previous studies, however, SIS conductance was computed numerically, and the universality of the amount of the jump at  $2\Delta$  was not discussed, although it is clearly seen in the numerical data.

We now turn to the main subject of the paper and discuss the forms of SIN and SIS conductances for strong spin-fermion interaction.

We first show that the features observed in a gas are in fact quite general and are present in an arbitrary Fermi liquid as long as the impurity scattering is weak. Indeed, in an arbitrary  $d$ -wave superconductor,

$$N(\omega) \propto \text{Im} \int d\phi \frac{\Sigma(\phi, \omega)}{(F^2(\phi, \omega) - \Sigma^2(\phi, \omega))^{1/2}}, \quad (3)$$

where  $\phi$  is the angle along the Fermi surface, and  $F(\phi, \omega)$  and  $\Sigma(\phi, \omega)$  are the retarded anomalous pairing vertex and retarded fermionic self-energy at the Fermi surface (the latter includes a bare  $\omega$  term in the fermionic propagator). The measured superconducting gap  $\Delta(\phi)$  is a solution of  $F(\phi, \Delta(\phi)) = \Sigma(\phi, \Delta(\phi))$ .

In the absence of impurity scattering,  $\text{Im} \Sigma$  and  $\text{Im} F$  in a superconductor both vanish at  $T=0$  up to a frequency which for arbitrary strong interaction exceeds  $\Delta$ . The Kramers-Kronig relation then yields at low frequencies  $\text{Re} \Sigma(\phi, \omega) \propto \omega$ ,  $\text{Re} F(\phi, \omega) \propto (\phi - \phi_{node})$ , where  $\phi_{node}$  is a position of the node of the  $d$ -wave gap. Substituting these forms into Eq. (3) and integrating over  $\phi$ , we obtain  $N(\omega) \propto \omega$  though the prefactor is different from that in a gas. The linear behavior of the DOS in turn gives rise to the quadratic behavior of the SIS conductance.

Similarly, expanding  $\Sigma^2 - F^2$  near each of the maxima of the gap we obtain  $\Sigma^2(\phi, \omega) - F^2(\phi, \omega) \propto (\omega - \Delta) + B(\phi - \phi_{max})^2$ , where  $B > 0$ . Then

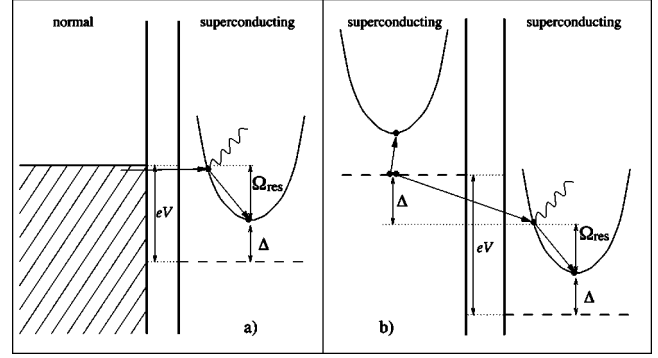


FIG. 2. The schematic diagram for the dip features in SIN and SIS tunneling conductances [(a) and (b), respectively]. For SIN tunneling, the electron which tunnels from a normal metal can emit a propagating spin wave if the voltage  $eV = \Delta + \Omega_{res}$ , where  $\Omega_{res}$  is the minimum frequency for spin excitations. After emitting a spin wave, the electron falls to the bottom of the band which leads to a sharp reduction of the current and produces a drop in  $dI/dV$ . For SIS tunneling, the physics is similar, but one first has to break an electron pair, which costs energy  $2\Delta$ .

$$N(\omega) \propto \text{Re} \int \frac{d\tilde{\phi}}{\sqrt{B\tilde{\phi}^2 + (\Omega - \Delta)}} \approx -\frac{\ln|\Omega - \Delta|}{\sqrt{B}}. \quad (4)$$

This result implies that the SIN conductance in an arbitrary Fermi liquid still has a logarithmic singularity at  $eV = \Delta$ , though its residue depends on the strength of the interaction. The logarithmical divergence of the DOS causes the discontinuity in the SIS conductance by the same reasons as in a Fermi gas.

In the presence of impurities, the logarithmical singularity is smeared out, and the DOS acquires a nonzero value at zero frequency (at least, in the self-consistent  $T$ -matrix approximation<sup>12</sup>). However, for small concentration of impurities, this affects the conductances only in narrow frequency regions near singularities while away from these regions the behavior is the same as in the absence of impurities.

We now show that a strong spin-fermion interaction gives rise to extra features in the SIS and SIN conductances not present in a gas. The qualitative explanation of these features is the following. At strong spin-fermion coupling, a  $d$ -wave superconductor possesses *propagating*, spin-wave type collective spin excitations near antiferromagnetic momentum  $Q$  and at frequencies below  $2\Delta$ . These excitations give rise to a sharp peak in the dynamical spin susceptibility at a frequency  $\Omega_{res} < 2\Delta$ ,<sup>9</sup> and also contribute to the damping of fermions near hot spots (points at the Fermi surface separated by  $Q$ ), where the spin-mediated  $d$ -wave superconducting gap is at maximum. If the voltage for SIN tunneling is such that  $eV = \Omega_{res} + \Delta$ , then an electron which tunnels from the normal metal can emit a spin excitation and fall to the bottom of the band [see Fig. 2(a)] losing its group velocity. This obviously leads to a sharp reduction of the current and produces a dip in  $dI/dV$ .

Similar effect holds for SIS tunneling. Here, however, one has to first break an electron pair, which costs the energy  $2\Delta$ . After a pair is broken, one of the electrons becomes a quasiparticle in a superconductor and takes an energy  $\Delta$ , while the other tunnels. If  $eV = 2\Delta + \Omega_{res}$ , the electron

which tunnels through a barrier has energy  $\Delta + \Omega_{res}$ , and can emit a spin excitation and fall to the bottom of the band. This again produces a sharp drop in  $dI/dV$  [see Fig. 2(b)].

In the rest of the paper we consider this effect in more detail and make quantitative predictions for the experiments. Our goal is to compute  $dI/dV$  for SIN and SIS tunneling for strong spin-fermion interaction.

The point of departure for our analysis is the set of two Eliashberg-type equations for the fermionic self-energy  $\tilde{\Sigma}_\omega$ , and the spin-polarization operator  $\Pi_\Omega$ . The latter is related to the dynamical spin susceptibility at the antiferromagnetic momentum by  $\chi^{-1}(Q, \Omega) \propto 1 - \Pi_\Omega$ . The same set was used in our earlier analysis of the relation between ARPES and neutron data.<sup>7</sup> In Matsubara frequencies these equations read ( $\tilde{\Sigma}_{\omega_m} = i\Sigma(\omega_m)$ )

$$\tilde{\Sigma}_{\omega_m} = \omega_m + \frac{3R}{8\pi^2} \int \frac{\tilde{\Sigma}_{\omega_m + \Omega_m}}{q_x^2 + \tilde{\Sigma}_{\omega_m + \Omega_m}^2 + F^2} \frac{d\Omega_m}{\sqrt{q_x^2 + 1 - \Pi_\Omega}},$$

$$\Pi_\Omega = \frac{1}{2} \int \frac{d\omega_m}{\omega_{sf}} \left( \frac{\tilde{\Sigma}_{\Omega_m + \omega_m} \tilde{\Sigma}_{\omega_m} + F^2}{\sqrt{\tilde{\Sigma}_{\Omega_m + \omega_m}^2 + F^2} \sqrt{\tilde{\Sigma}_{\omega_m}^2 + F^2}} - 1 \right). \quad (5)$$

This set is a simplification of the full set of Eliashberg equations that includes also the equation for the anomalous vertex  $F(\omega)$ .<sup>13</sup> As in Ref. 7 we assume that near optimal doping, the frequency dependence of  $F(\omega)$  is weak at  $\omega \sim \Delta$  relevant to our analysis, and replace  $F(\omega)$  by a frequency independent input parameter  $F$ . Other input parameters in Eq. (5) are the dimensionless coupling constant  $R = \bar{g}/(v_F \xi^{-1})$  and a typical spin-fluctuation frequency  $\omega_{sf} = (\pi/4)(v_F \xi^{-1})^2/\bar{g}$ . They are expressed in terms of the effective spin-fermion coupling constant  $\bar{g}$ , the Fermi velocity at a hot spot  $v_F$ , and the magnetic correlation length  $\xi$ . By all accounts, at and below optimal doping,  $R \geq 1$ ,<sup>14</sup> i.e., the system behavior falls into the strong coupling regime.

Strictly speaking, the set (5) is valid near hot spots where  $\phi \approx \phi_{max}$ . Away from hot spots  $F(\phi)$  is reduced compared to  $F$ . We, however, will demonstrate that the additional features due to spin-fermion interaction are produced solely by fermions from hot regions.

As in Ref. 7, we consider the solution of Eq. (5) for the experimentally relevant case  $F \gg R\omega_{sf}$  when the measured superconducting gap  $\Delta \sim F^2/(R^2\omega_{sf}) \gg \omega_{sf}$ . In this situation, at frequencies  $\sim \Delta$ , fermionic excitations in the normal state are overdamped due to strong spin-fermion interaction. In a superconducting state, the form of the spin propagator is modified at low frequencies because of the gap opening, and this gives rise to a strong feedback from superconductivity on the electron DOS.

More specifically, we argued in Ref. 7 that in a superconductor,  $\Pi_\Omega$  at low frequencies  $\Omega \ll 2\Delta$  behaves as  $\Omega^2/\Delta$ , i.e., collective spin excitations are undamped, propagating spin waves. This behavior is peculiar to a superconductor — in the normal state, the spin excitations are completely overdamped. The propagating excitations give rise to the reso-

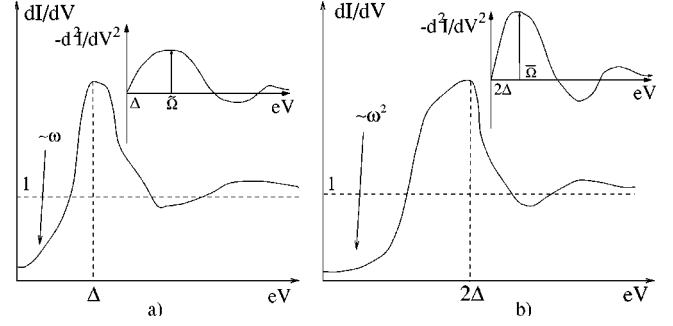


FIG. 3. The schematic forms of SIN (a) and SIS (b) tunneling conductances for strong spin-fermion interaction. We added small impurity scattering to soften singular features related to the sharpness of the Fermi surface (see the text). The dip/hump features above the peaks are the strong coupling effects not present in a gas. The insets show the derivatives of conductances above  $\Delta$  for SIN tunneling and  $2\Delta$  for SIS tunneling. We argue in the text that these derivatives have maxima at voltages  $eV = \tilde{\Omega} = \Delta + \Omega_{res}$  for SIN tunneling and  $eV = \bar{\Omega} = 2\Delta + \Omega_{res}$  for SIS tunneling, where  $\Omega_{res}$  is the resonance spin frequency measured in neutron experiments.

nance in  $\chi(Q, \Omega)$  at  $\Omega_{res} \sim (\Delta\omega_{sf})^{1/2} \ll \omega_{sf}$ , where  $\text{Re} \Pi(\Omega_{res}) = 1$ .<sup>7</sup> This resonance accounts for the peak in neutron scattering.<sup>9</sup>

The presence of a new magnetic propagating mode changes the electronic self-energy for electrons near hot spots. In the absence of a propagating mode, an electron can decay only if its energy exceeds  $3\Delta$ . Due to resonance, an electron at a hot spot can emit a spin wave already when its energy exceeds  $\Delta + \Omega_{res}$ . It is essential that contrary to a conventional electron-electron scattering, this process gives rise to a discontinuity in  $\text{Im} \Sigma(\omega)$  at the threshold. Indeed, using the spectral representation to transform from Matsubara to real frequencies in the first equation in Eq. (5), integrating over momentum and neglecting for simplicity unessential  $q_x^2$  in the spin susceptibility, we obtain for  $\omega \geq \omega_{th} = \Delta + \Omega_{res}$

$$\text{Im} \Sigma(\omega) \propto \int_{\Omega_{res}}^{\omega - \Delta} d\Omega \frac{1}{\sqrt{\omega - \Omega - \Delta}} \frac{1}{\sqrt{\Omega - \Omega_{res}}}$$

$$\propto \int_0^{(\omega - \omega_{th})^{1/2}} dx \frac{1}{\sqrt{\omega - \omega_{th} - x^2}} = \frac{\pi}{2}. \quad (6)$$

We see that  $\text{Im} \Sigma(\omega)$  jumps to a finite value at the threshold. This discontinuity is peculiar to two dimensions. By Kramers-Kronig relation, the discontinuity in  $\text{Im} \Sigma$  gives rise to a logarithmical divergence of  $\text{Re} \Sigma$  at  $\omega = \omega_{th}$ . This in turn gives rise to a vanishing spectral function near hot spots, and accounts for a sharp dip in the ARPES data.<sup>8</sup>

We now show that the singularity in  $\text{Re} \Sigma(\omega)$  causes the singularity in the derivatives over voltages of both SIN and SIS conductances  $d^2I/dV^2$ . Indeed, near a hot spot,  $F(\phi) = F(1 - \lambda \tilde{\phi}^2)$ , where  $\tilde{\phi} = \phi - \phi_{max}$ , and  $\lambda > 0$ . Then, quite generally,  $\text{Re} \Sigma(\phi, \omega) \propto \ln|\omega - \omega_{th}(\phi)|$ , where  $\omega_{th}(\phi) = \omega_{th} + C\tilde{\phi}^2$ , and  $C > 0$ . Substituting this expression into the DOS and differentiating over frequency, we obtain after a simple algebra

$$\begin{aligned} \frac{\partial N(\omega)}{\partial \omega} &\sim - \int \frac{F^2(\phi)}{\Sigma^3(\phi, \omega)} \partial_\omega \Sigma(\phi, \omega) d\phi \\ &\sim \frac{1}{\ln^3 |\omega - \omega_{th}|} \frac{\Theta(\omega_{th} - \omega)}{\sqrt{\omega_{th} - \omega}}, \end{aligned} \quad (7)$$

where  $\Theta(x)$  is a step function. We see that  $\partial N(\omega)/\partial \omega$  has a one-sided, square-root singularity at  $\omega = \omega_{th}$ . Physically, this implies that the conductance drops when propagating electrons start emitting spin excitations. Note that the typical  $\phi$  which contribute to the singularity are small (of order  $|\omega_{th} - \omega|^{1/2}$ ), which justifies our assertion that the singularity is confined to hot spots.

The singularity in  $\partial N(\omega)/\partial \omega$  is likely to give rise to a dip in  $N(\omega)$  at  $\omega \geq \omega_{th}$ . The argument here is based on the fact that if the angular dependence of  $\omega_{th}(\phi)$  is weak (i.e.,  $C$  is small), then  $\Sigma(\omega_{th}) \gg F(\omega_{th})$ , and  $N(\omega_{th})$  reaches its normal-state value with infinite negative derivative. Obviously then, at  $\omega > \omega_{th}$ ,  $N(\omega)$  goes below its value in the normal state and should therefore have a minimum at some  $\omega \geq \omega_{th}$ . Furthermore, at larger frequencies, we solved Eq. (5) perturbatively in  $F(\omega)$  and found that  $N(\omega)$  approaches a normal-state value *from above*. This implies that besides a dip,  $N(\omega)$  should also display a hump somewhere above  $\omega_{th}$ . The behavior of the SIN conductance is schematically shown in Fig. 3(a).

Similar results hold for SIS tunneling. The derivative of the SIS current,  $d^2 I/dV^2 \sim \partial G(\omega)/\partial \omega$ , is given by

$$\frac{\partial G(\omega)}{\partial \omega} = \int_0^\omega \partial_\omega N(\omega - \Omega) \partial_\Omega N(\Omega) d\Omega. \quad (8)$$

Evaluating the integral in the same way as for SIN tunneling, we find a square-root singularity at  $\omega = \omega_{th}^* = 2\Delta + \Omega_{res}$

$$\begin{aligned} \frac{d^2 I}{dV^2} &\sim -P \int_0^\omega \frac{d\Omega}{\omega - \Omega - \Delta} \frac{1}{\ln^3 |\omega_{th} - \Omega|} \frac{\Theta(\omega_{th} - \omega)}{\sqrt{\omega_{th} - \omega}} \\ &\sim - \frac{1}{\ln^3 |\omega_{th}^* - \omega|} \frac{\Theta(\omega_{th}^* - \omega)}{\sqrt{\omega_{th}^* - \omega}}. \end{aligned} \quad (9)$$

The singularity comes from the region where  $\Omega \approx \omega_{th}$  and  $\omega - \Omega \approx \Delta$ , and both  $\partial_\omega N(\omega - \Omega)$  and  $\partial_\Omega N(\Omega)$  are singular.

Again, it is very plausible that the singularity of the derivative causes a dip at a frequency  $\omega \geq \omega_{th}^*$ , and a hump at even larger frequency. We stress, however, that at exactly  $\omega_{th}^*$ , the SIS conductance has an infinite derivative, while the dip occurs at a frequency which is somewhat larger than  $\omega_{th}^*$ . The behavior of the SIS conductance is presented in Fig. 3.

Qualitatively, the forms of conductances presented in Fig. 3 agree with the SIN and SIS data for YBCO and Bi2212 materials.<sup>1,2</sup> Moreover, recent SIS tunneling data for Bi2212<sup>2</sup> indicate that the relative distance between the peak and the dip [ $\Omega_{res}/(2\Delta)$  in our theory] decreases with underdoping. More data analysis is, however, necessary to quantitatively compare tunneling and neutron data.

To summarize, in this paper we considered the forms of SIN and SIS conductances both for noninteracting fermions, and for fermions which strongly interact with their own collective spin degrees of freedom. We argue that for strong spin-fermion interaction, the resonance spin frequency  $\Omega_{res}$  measured in neutron scattering can be inferred from the tunneling data by analyzing the derivatives of SIN and SIS conductances. We found that the derivative of the SIN conductance diverges at  $eV = \Delta + \Omega_{res}$  while the derivative of the SIS conductance diverges at  $eV = 2\Delta + \Omega_{res}$ , where  $\Delta$  is the maximum value of the  $d$ -wave gap.

It is our pleasure to thank G. Blumberg, A. Finkel'stein, and particularly J. Zasadzinski for useful conversations. The research was supported by NSF Contract No. DMR-9979749.

<sup>1</sup>Ch. Renner *et al.*, Phys. Rev. Lett. **80**, 149 (1998); Y. DeWilde *et al.*, *ibid.* **80**, 153 (1998).

<sup>2</sup>N. Miyakawa *et al.*, Phys. Rev. Lett. **83**, 1018 (1999); L. Ozyurer, J.F. Zasadzinski, and N. Miyakawa, cond-mat/9906205 (unpublished); J.F. Zasadzinski (private communication).

<sup>3</sup>G.D. Mahan, *Many-Particle Physics* (Plenum Press, New York, 1990).

<sup>4</sup>J.P. Carbotte, Rev. Mod. Phys. **62**, 1027 (1990), and references therein.

<sup>5</sup>D.Z. Liu, Y. Zha, and K. Levin, Phys. Rev. Lett. **75**, 4130 (1995); I. Mazin and V. Yakovenko, *ibid.* **75**, 4134 (1995); A. J. Millis and H. Monien, Phys. Rev. B **54**, 16 172 (1996); N. Bulut and D.J. Scalapino, *ibid.* **53**, 5149 (1996); Z-X Shen and J.R. Schrieffer, Phys. Rev. Lett. **78**, 1771 (1997); M.R. Norman and R. Ding, Phys. Rev. B **57**, R11 089 (1998).

<sup>6</sup>Ph. Monthoux and D. Pines, Phys. Rev. B **47**, 6069 (1993); D.J.

Scalapino, Phys. Rep. **250**, 329 (1995).

<sup>7</sup>Ar. Abanov and A.V. Chubukov, Phys. Rev. Lett. **83**, 1652 (1999).

<sup>8</sup>J.C. Campuzano *et al.*, Nature (London) **392**, 157 (1988); Z-X. Shen *et al.*, Science **280**, 259 (1998).

<sup>9</sup>H.F. Fong *et al.*, Phys. Rev. B **54**, 6708 (1996); P. Dai *et al.*, Science **284**, 1344 (1999).

<sup>10</sup>M.R. Norman *et al.*, Phys. Rev. Lett. **79**, 3506 (1997).

<sup>11</sup>H. Won and K. Maki, Phys. Rev. B **49**, 1397 (1994).

<sup>12</sup>P.J. Hirschfeld, P. Wolfle, and D. Einzel, Phys. Rev. B **37**, 83 (1988); T.P. Devereaux and A.P. Kampf, Int. J. Mod. Phys. **11**, 2093 (1997) and references therein.

<sup>13</sup>Ar. Abanov, A. Chubukov, and A.M. Finkel'stein, cond-mat/9911445 (unpublished).

<sup>14</sup>A. Chubukov, Europhys. Lett. **44**, 655 (1997).